© 2018 IJSRST | Volume 4 | Issue 5 | Print ISSN: 2395-6011 | Online ISSN: 2395-602X
Themed Section: Science and Technology

Synthesis, Structural and Optical Behavior of Cerium Oxide Nanoparticles by Co-Precipitation Method

N.Ramjeyanthi[1*], M.Alagar[2], D.Muthuraman[3]

[*1]Department of Physics, PSN College of Engineering & Technology, Tirunelveli, Tamil Nadu, India

[2]Centre for Research and Post Graduate Studies, Department of Physics, Ayyanadar Janakiammal College, Sivakasi, Tamil Nadu, India

[3]Department of Physics, PSN College of Engineering & Technology, Tirunelveli, Tamil Nadu, India

ABSTRACT

In this paper, cerium oxide (CeO_2) nanoparticles were synthesized by co-precipitation method and validate its physical, chemical and optical properties. X-ray diffraction (XRD) pattern confirms the formation of cubic fluorite structured CeO_2 nanoparticles with Fm3 space group. Comparative study for crystallite size of CeO_2 nanoparticles was realized with the help of Debye-Scherer's method and Williamson-Hall (W-H) plot analysis. The appearance of Ce-O stretching band in the Fourier transformed infrared (FTIR) spectrum confirms the formation of CeO_2 nanoparticles. Scanning electron microscopy (SEM) results exposed the formation of spherical shaped particles with nanosize regime. Optical properties of CeO_2 nanoparticles were analyzed from UV-visible diffuse reflectance spectroscopy and the direct band gap value was found to be 3.30 eV. Photoluminescence (PL) spectrum display the broad emission peak in the wavelength ranges of 450-495 nm under the excitation of 325 nm.

Keywords: CeO_2, Nanoparticles, co-precipitation, crystallite size, optical properties

I. INTRODUCTION

Recently, rare earth oxide nanoparticles are attracted for their many applications due to their interesting structural and optical properties with outstanding luminescence efficiency in the visible region [1, 2]. Luminescence behavior of rare earth oxides is mainly originates from the partially-filled 4f electronic shell.

Amongst rare earth oxides, cerium oxide (CeO_2) nanoparticles are interesting materials for many potential applications such as solid state electrolyte for electrochemical devices [3], catalyst for automobile exhauster [4], sun screen for UV absorbents [5], luminescent materials [6], gas sensors [7], polishing materials [8], and oxygen storage capacity [9]. Since, CeO_2 nanoparticles offer many active sites for free radicals scavenging because of their large surface to volume ratio and their mixed valence states for unique redox chemistry [10]. Moreover, the crystallites with nanosize regime can be easy to confine the movement of phonons. In earlier days, CeO_2 nanoparticles have been prepared by several synthesis techniques such as sol-gel [11], chemical precipitation [12], thermal decomposition [13], hydrothermal [14], and combustion method [15]. Among these, co-precipitation offers many advantages include the simple process, low cost, and the crystallization degree and particle size of powders are controllable [16].

In this regard, CeO_2 nanoparticles were prepared from the co-precipitation method by using the cerium

nitrate hexahydrate ($Ce(NO_3)_3.6H_2O$) as a precursor and sodium hydroxide (NaOH) can act as a chelating agent. Furthermore, the physical, chemical, morphological and optical properties of obtained CeO_2 nanoparticles were characterized by using the XRD, FTIR, SEM, UV-Visible DRS and PL analytical tools respectively.

II. METHODS AND MATERIAL

A. Materials

Cerium (III) nitrate hexahydrate ($Ce(NO_3)_3.6H_2O$ (434.22 g/mole; 99.9% purity) and Sodium hydroxide (NaOH) (40.00 g/mole; 99.9% purity) were purchased from Himedia Laboratories Pvt. Ltd. These chemicals were used without any further purification. Distilled water and ethanol were used for solvent and washing process.

B. Synthesis of CeO_2 nanoparticles

0.1 M of cerium nitrate was dissolved in distilled water with constant stirring for 30 minutes at room temperature. Afterwards, 0.3 M aqueous NaOH solution was added to the cerium nitrate solutions by drop-wise at room temperature with constant stirrer and allows to the settle down of solution. An un-reacted nitrate present in the resultant precursor solution was completely removed by washing process with the help of water and ethanol in several times. During this washing process, appearance of the final precursor solution was changes from dark blackish into whitish color. The final product was filtered and dried at room temperature for 96 hours. At last, obtained powder samples were grained by using mortar and pestle and obtain the ultrafine CeO_2 nanoparticles.

III. RESULTS AND DISCUSSION

A. XRD analysis

The crystalline behavior of as prepared CeO_2 sample was characterized by X-ray diffraction (XRD) in the diffraction angle (2Θ) ranges between 10º and 80º with scanning rate of 5º per minute. The XRD pattern of as prepared CeO2 sample is shown in Fig. 1(a). The obtained results shows that the maximum intensity peak was observed at (111) and other intensity peaks were observed at (200), (220), (311), (222), (400), (331), and (420) crystal planes. All the identified peaks are good agreement with the JCPDS file (34-0394) and well consistent with earlier report [17]. It clearly indicates the formation of polycrystalline CeO_2 (space group: Fm3m) with cubic fluorite structure.

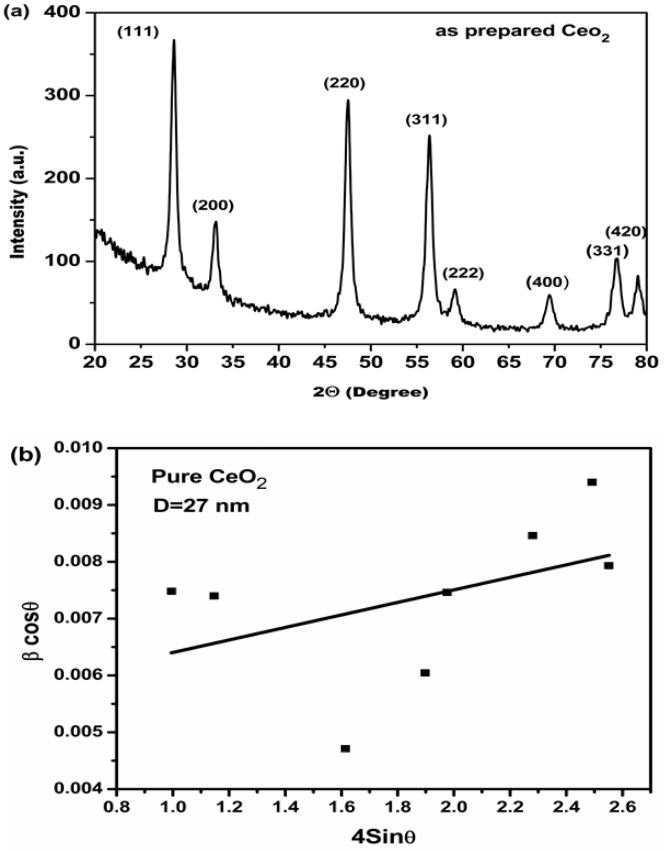

Figure 1. (a) XRD Pattern (b) W-H Plot of the as prepared CeO_2 nanoparticles

The average crystallite size (D in nm) of the CeO_2 nanoparticles was found to be 21 nm by using the Debye-Scherrer formula [18] as follows,

$$D = K\lambda/\beta\cos\theta$$

Where K is a constant (0.89), λ is the wavelength of X-ray (λ=1.5418Å), θ is the diffraction angle for the peak and β is full width at half maximum (FWHM). Taking in to the account of instrumental broadening, average

crystallite size of CeO_2 nanoparticles also calculated by using Williamson-Hall plot analysis [19]. Fig. 1(b) illustrates the W-H plot for CeO_2 nanoparticles. From this plot, the crystallite size of CeO_2 nanoparticles was found to be 27 nm. The crystallite size observed from the W-H method is slightly high compared to the size measured from the Debye-Scherrer method. It may ascribe to be removal of broadening error was achieved in the W-H plot. In addition to the crystallographic parameters of as prepared CeO_2 nanoparticles were summarized in Table 1.

Table 1. Crystallographic properties of as prepared CeO_2 nanoparticles

Lattice Parameter (a=b=c) (Å)	Unitcell Volume (V) (Å)³	Average Crystallite size (nm)	
		Debye-Scherrer method	Williamson-Hall method
5.4033	157.75	21	27

B. FTIR Spectra analysis

The functional group of as synthesized CeO_2 nanoparticles was analyzed by using FTIR spectroscopy. FTIR spectra (Fig. 2) of CeO_2 nanoparticles were measured in the wave number range of 400 to 4000 cm-1. The obtained bands were good agreement with the literature [20, 21]. A strong absorption band at 3400 and 1632 cm^{-1} represents the water and hydroxyl stretches (O-H stretching). The bands observed 2925 and 2848 cm^{-1} are arising due to C-H bonding. The band at 2365 and 1399 cm^{-1} may appear from the absorption of atmospheric CO_2. The absorption band at 855, 743 and 614 cm^{-1} represent the metal-oxygen Stretching (Ce-O stretch) which confirm the formation of CeO_2 nanoparticles.

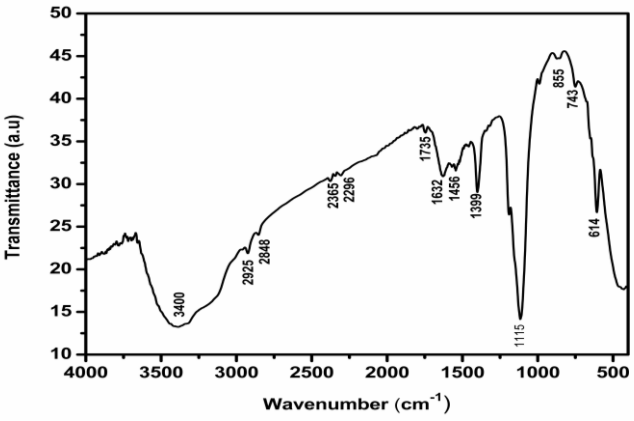

Figure 2. FTIR Spectra of as prepared CeO_2 nanoparticles

C. SEM analysis

Scanning electron microscope (SEM) is the powerful magnification tool to detect surface morphology of nanoparticles. The obtained SEM image of the as prepared CeO_2 nanoparticles was shown in Fig. 3. It evident that the surface of CeO_2 consists of spherical shaped particles with homogenous distribution. Apart from this some less number of agglomerations was also identified in the SEM images. The obtained morphology was also well connected with Literature [21, 22]. Due to the greater agglomerations, an exact value of particle size was not easy to calculate. An approximate value of average particle size was found to be 45 nm by using the ImageJ software.

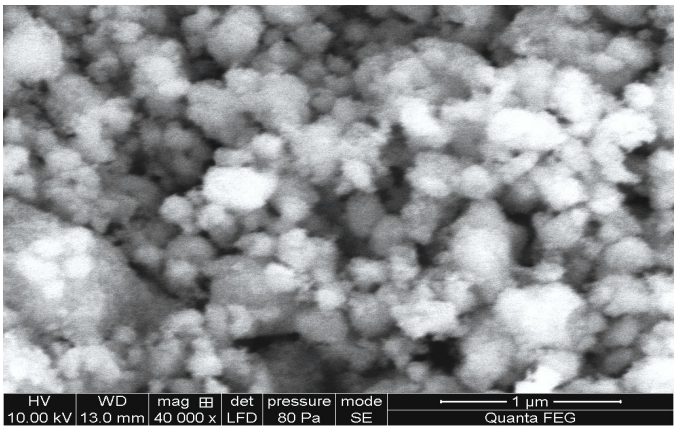

Figure 3. SEM image of the as prepared CeO_2 nanoparticles

D. UV-Vis DRS spectra analysis

The optical behavior of as prepared CeO_2 nanoparticles was analysed by using UV visible diffuse reflectance spectroscopy.

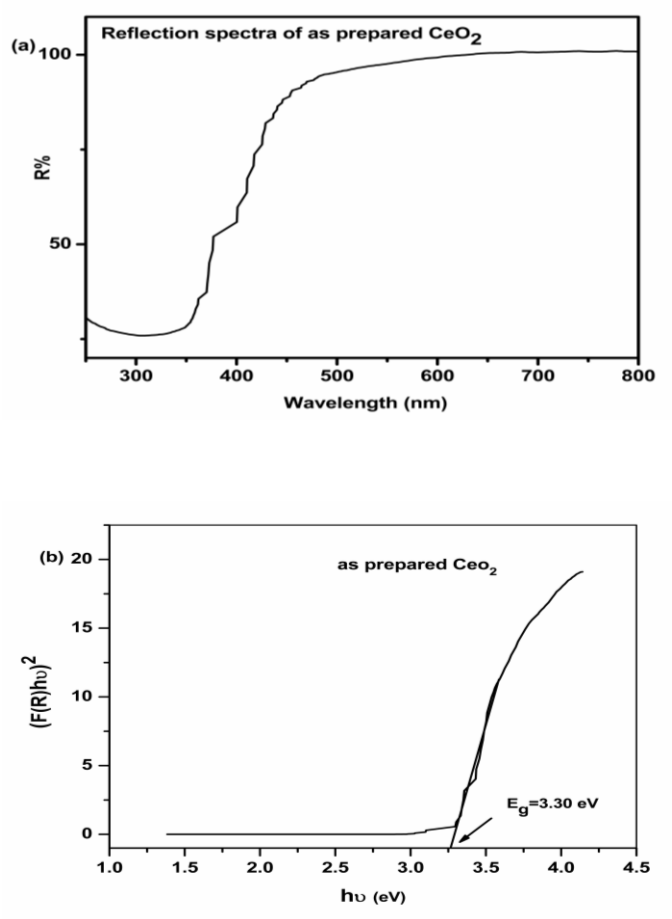

Figure 4. Room temperature (a) optical reflectance spectra and (b) K-M Plot of CeO_2 nanoparticles

The reflectance spectra of CeO_2 nanoparticle was shown in Fig. 4(a). From this data, the direct band gap value of CeO_2 nanoparticles was calculated by using Kubelka-Munk (K-M method) equation [23, 24],

$$(h\upsilon\ F(R))^2 = A(h\upsilon - Eg)$$

where $F(R) = (1-R)^2/2R$, h is a Planks constant, υ is the light frequency, A is the absorption coefficient and E_g is the band gap energy. The K-M plot was drawn between $(h\upsilon\ F(R))^2$ and hυ as shown in Fig. 4(b). A straight line is drawn tangent to the point of interaction with hυ axis which gives the bandgap energy value 3.30 eV. The obtained E_g value shows that blue shift occur on the CeO_2 nanoparticles. The attained bandgap value was concord with literature [25].

E. PL spectra analysis

The electronic structure of as prepared CeO_2 nanoparticles was examined by using Photoluminescence (PL) spectroscopy. Compared to other optical characterization tools PL is the more leading technique to find optical properties of the material without destructing the sample. The obtained PL spectra of CeO_2 nanoparticles in the wavelength range of 330-900 nm was recorded under the excitation of 325 nm. The PL spectra of CeO_2 nanoparticles (Fig .5) exhibits a fine UV emission at 358nm (3.47 eV) and four visible emission peaks 452 nm (2.74 eV), 469 nm (2.64 eV), 483 nm (2.57 eV), 493 nm (2.52 eV) observed in the blue region. Apart from this, strong green emission was also observed at 574 nm (2.16 eV). The emission band observed in the wavelength from 358 to 574 nm is originates from the relative oxygen vacancies (surface defects) of CeO_2 nanoparticles. It may causes from the changes in particle size. The relative oxygen vacancies can be also explained on the basis of transfer of charge carrier between 4f conduction band (Ce) to the 2p valance band (O) of CeO_2 nanoparticles. This result is similar to the earlier reports [26, 27].

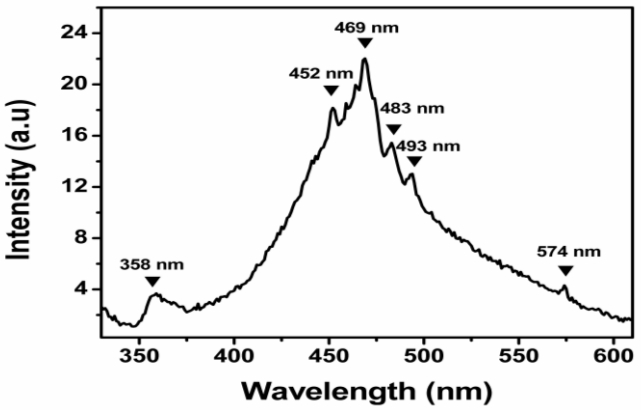

Figure 5. Room temperature PL spectra of CeO_2 nanoparticles

IV. CONCLUSION

Ultrafine cerium oxide nanoparticles were successfully synthesized by co-precipitation method at room temperature. The cubic phase of the CeO_2 nanoparticles were confirmed from XRD pattern and crystallite size of the particles is found to be 21 nm (Scherrer method) and 27 nm (W-H Plot). The SEM images of CeO_2 nanoparticles shows that the particles are spherical in shape with less number of agglomerations. The strong absorption band identified in the wavelength of 325 nm indicates that the CeO_2 nanoparticles have high UV absorption characteristics. The PL spectrum indicates the CeO_2 nanoparticles having the violet-blue light emission.

V. REFERENCES

[1]. G. Adachi, N. Imanka, Z. C. Kang, "Binary rare earth oxides", Kluwer Academic Publishers, Newyork (2004).

[2]. A. Kitai, "Luminescent material and application", John Wiley & Sons Ltd,Canada (2008) .

[3]. M. Mogensen, N. M Sammes, G. A Tompsatt, Solid State Ionics, 129 (2000) 63-94.

[4]. O. Zawam, Journal Alloys Compounds, 886 (1998) 275-277.

[5]. J. F. D. Lima, R. F. Martins, C. R. Neri, O. A. Serra, Applied Surface Science, 255 (2009) 9006-9009.

[6]. X. J. Yu, P. B. Xie, Q. D. Su, Physical Chemistry Chemical Physics, 3 (2001) 5266-5269.

[7]. N. Izu, W. Shin, N. Murayama, S. Kanzaki, Sensors and Actuators B, 87 (2002) 95-104.

[8]. S. H. Lee, Z. Y. Lu, S. V. Babu, E. Matijevic, Material Research, 17 (2002) 2744-2749.

[9]. N. Kakuta, N. Morishima, M. Kotobuki, T. Iwase, T. Mizushima, Y. Sato, S. Matsuura, Applied Surface Science, 121- 122 (1997) 408-412.

[10]. R. J. Hunter, V. R. Preedy, "Nanomedicine in Health and Disease", CRC Press, (2017) 271-272.

[11]. M Alifanti, B. Baps, N. Blangenois, Chemical material, 15 (2003) 395-403.

[12]. H.R. Pouretedal, A. Kadhodaie, Chinese Journal of Catalysis, 31 (2010) 1328-1334.

[13]. Y. Wang, T. Mori, J. Li, T. Ikegami, Journal of American Ceramic Society, 85 (2002) 3105-3107.

[14]. S. Phoka, S. Pinisoontorn, P. Chirawatkul, Y. Poo-arporn, S. Maensir, Nanoscale Research letters, 7 (2012) 425-443.

[15]. S. Bojana, A. Zeljka, A. Nadica, K. Radenka, M. Mitric, M. Ametia, D.D. Miroslav, Acta Chimica Slovenica, 55 (2008) 486-491.

[16]. J. Luo, J. Chen, W. Li, Z. Huang, C. Chen, MATEC Web of Conferences, 26 (2015) 01007-01007-5.

[17]. G. Wang, Q. Mu, T. Chen, Y. Wangi, Journal of alloy and compounds , 493 (2010) 202-207.

[18]. H. Chang, H. Chen, Journal of Crystal Growth 283 (2005) 457-461.

[19]. G. K. Williamson, W. Hall, Acta Metallurgica, 1 (1953) 22-31.

[20]. S. Phoka, P. Laokul, E. Swatsitang, V. Promarak, S. Seraphin, S. Maensir, Material chemistry and Physics 115 (2009) 423-428.

[21]. E. Kumar, P. Selvarajan, K. Balasubramanian, Recent Research in Science and technology, 2(4) 2010 37-41.

[22]. M. Chelliah, J.B. Rayappan, U. Krishnan, Journal of Applied Sciences 12(16) (2012)1734-1737.

[23]. P. Kubelka, F. Munk Z Tech phys 12 (1931) 593-601.

[24]. P. Kubelka Journal of the Optical Society of America B, 38 (1948) 448-457

[25]. D. M. D. Prabaharan, K. Sadaiyandi, M. Mahendran, S. Sagadevan, Materials Research, 19(2) (2016) 478-482.

[26]. M. A. Majeedk khan, W. Khan, M. Ahamed, A.Alhazaa, Scientific reports, (2017) 25-32.

[27]. K. K. Babitha, A. Sreedevi, K. P. Priyanka, B. Sabu, T. Varghese, Indian Journal of pure & Applied Physics, 53 (2015) 596-603